*Article*

# Photocatalytic Performance of a Novel MOF/BiFeO$_3$ Composite

**Yunhui Si [1], Yayun Li [1,*], Jizhao Zou [1], Xinbo Xiong [1], Xierong Zeng [1] and Ji Zhou [2]**

[1]  Shenzhen Key Laboratory of Special Functional Materials & Shenzhen Engineering Laboratory for Advance Technology of Ceramics, College of Materials Science and Engineering, Shenzhen University, Shenzhen 518060, China; 2161120218@email.szu.edu.cn (Y.S.); zoujizhao@szu.edu.cn (J.Z.); xxbszdx@szu.edu.cn (X.X.); zengxier@szu.edu.cn (X.Z.)

[2]  State Key Laboratory of New Ceramics and Fine Processing, School of Materials Science and Engineering, Tsinghua University, Beijing 100084, China; zhouji@tsinghua.edu.cn

*  Correspondence: kittyli@szu.edu.cn

**Abstract:** In this study, MOF/BiFeO$_3$ composite (MOF, metal-organic framework) has been synthesized successfully through a one-pot hydrothermal method. The MOF/BiFeO$_3$ composite samples, pure MOF samples and BiFeO$_3$ samples were characterized by X-ray diffraction (XRD), scanning electron microscopy (SEM), energy dispersive spectroscopy (EDS), and by UV–vis spectrophotometry. The results and analysis reveal that MOF/BiFeO$_3$ composite has better photocatalytic behavior for methylene blue (MB) compared to pure MOF and pure BiFeO$_3$. The enhancement of photocatalytic performance should be due to the introduction of MOF change the surface morphology of BiFeO$_3$, which will increase the contact area with MB. This composing strategy of MOF/BiFeO$_3$ composite may bring new insight into the designing of highly efficient photocatalysts.

**Keywords:** MOF; BiFeO$_3$; photocatalysts; morphology

## 1. Introduction

In the past few decades, much attention has been paid to semi-conductor photocatalysts for their potential utilization of solar energy to solve the increasing environmental and energy crisis [1]. As a first generation photocatalyst, TiO$_2$ has attracted the attention of many scientists. In the 1970s, the photocatalytic properties of TiO$_2$ were investigated [2]. Due to its high photocatalytic performance, non-toxicity, low cost, and ease of preparation, TiO$_2$ has been widely used in water pollution control and hydrogen production by decomposition of water. However, TiO$_2$ based photocatalysts are limited by the UV band due to their wide band gap defects [3], and can hardly utilize visible light. While ultraviolet light accounts for less than 5% of sunlight, the utilization efficiency of solar light limits the practical application of TiO$_2$ as a photocatalyst. With a narrow band gap of ~2.2 ev and excellent chemical stability, BiFeO$_3$ has good response in the visible light range and higher photocatalytic efficiency compared to TiO$_2$ based photocatalyst [4]. However, the high recombination rate of photogenerated electrons and holes, poor adsorption, and short lifetime of carriers result in lower photocatalytic activity of pure BiFeO$_3$. At present, measures to improve the photocatalytic performance of BiFeO$_3$ mainly include adjusting the size and morphology by changing the process [5], ion doping of rare earth elements [6], and surface deposition of noble metals [7]. To some extent, doping of rare earth ions can reduce the band gap of BiFeO$_3$ and increase photocatalytic activity [8,9]. However, the complete catalytic activity considerably depends upon surface adsorption over the surface of the photocatalyst [10–12]. A great deal of research on the modification of BiFeO$_3$ does not improve its adsorption performance significantly. In general, porous materials with different pore

sizes have a strong adsorption capacity, which has aroused our interest. Up until now, compositing $BiFeO_3$ with porous materials has scarcely been reported.

Metal-organic framework materials (MOFs) have the advantages of ordered pore structure, large specific surface area, and adjustable pore shape and size, their adsorption capacity is much higher than that of conventional adsorbents (such as molecular sieves and activated carbon) [13,14]. ZIF-8, 2-Methylimidazole zinc salt, one of the most widely studied zeolitic imidazolate framework materials, not only has the advantages of the above MOFs, but also has better hydrothermal stability [15], which gives it potential to couple with $BiFeO_3$. Benefitting from the diversity of the MOF species, this strategy of $MOF/BiFeO_3$ composite would provide new ideas for the designing of highly efficient photocatalysts.

In this work, MOF and $BiFeO_3$ composite photocatalyst was successfully synthesized by a simple and low cost hydrothermal process. Photodegradation experiments showed that the composite photocatalyst can effectively improve the photocatalytic ability of degrading organic dye compared with the pure $BiFeO_3$ and pure MOF.

## 2. Experimental Section

### 2.1. Preparation of MOF

For synthesis of ZIF-8, 0.744 g (2.50 mmol) $Zn(NO_3)_2 \cdot 6H_2O$ was dissolved in 100 mL methanol, 0.410 g (5 mmoL) 2-Methylimidazole was dissolved in 160 mL methanol respectively, stirring until fully dissolved. Then the two solutions were mixed by magnetic stirring, the molar ratio of the various components in the mixed solution was maintained at: $Zn^{2+}$:2-Methylimidazole = 1:2. The whole operation was carried out at room temperature without any heating. The solution was stirred with a constant speed at 800 r/min for 1 h, changed from transparent to ivory-white completely. The synthesized powder was washed by methanol and collected by centrifuging, then dried for 12 h in the fume hood.

### 2.2. Preparation of MOF/BiFeO₃ Composite

The preparation of $BiFeO_3$ powder by hydrothermal method has the advantages of controllable morphology, high purity, and small particle size distribution [16]. For synthesis of $MOF/BiFeO_3$ composite, $Fe(NO_3)_3 \cdot 9H_2O$ and $Bi(NO_3)_3 \cdot 5H_2O$ were added into deionized water with a molar ratio of 1:1. Then it was mixed with 1 mL nitric acid (68 wt %) and 2 g Polyethylene glycol (PEG-2000) by constant stirring at room temperature. 40 mL of KOH (12 M) solution used as a mineralizer was added dropwise into the mixed solution as slowly as possible. When the pH value of the solution was neutral, 0.3 g of prepared ZIF-8 powder was added. Subsequently, the mixture was transferred into a 50 mL Teflon lined stainless vessel, and heated at 180 °C for 24 h. After nature cooling, the obtained sample was centrifuged and thoroughly washed with deionized water. Finally, the $MOF/BiFeO_3$ composite was dried at 80 °C in a vacuum oven for 14 h.

### 2.3. Characterization of Phase and Microstructure

The phase compositions were characterized by X-ray powder diffraction (D8Advance, Karlsruhe, Germany) with a graphite monochromator and Cu K$\alpha$ ($\lambda$ = 0.15418 nm) radiation operating at 40 kV and 200 mA. The microstructural morphologies of the $MOF/BiFeO_3$ composite were observed via scanning electron microscopy (Hitachi SU70, Tokyo, Japan).

### 2.4. Measurements of Photocatalytic Performance

The photocatalytic performance of pure $BiFeO_3$, pure MOF, and $MOF/BiFeO_3$ photocatalysts were evaluated by the degradation of Methylene blue (MB) with a concentration of 20 mg/L in aqueous solution under visible light irradiation (Xe lamp, 300 W; visible cut off filter >420 nm). Methylene blue is a cationic dye with a methyl nitride group $[(CH_3)_2N^+]$. In order to prevent any thermal catalytic

effect, the reaction temperature was kept at 20 °C by circulation water during the whole process. For intuitive contrast, 30 mg of samples were applied to photocatalytic experiments. The samples and 80 mL MB solution (20 mg/L) were placed in a reactor, and the suspension was placed in the dark and magnetically stirred for 30 min to reach the adsorption/desorption equilibrium before light irradiation. The degradation of MB was examined using a spectrophotometer (Shimadzu UV-2450, Kyoto, Japan) by centrifuging the retrieved samples and measuring the intensity of the absorption peak of MB (663 nm) relative to its initial value ($C/C_0$) at intervals of 20 min.

## 3. Results and Discussion

### 3.1. X-ray Diffraction Analysis

Figure 1 shows the X-ray diffraction (XRD) patterns of (a) simulated MOF (ZIF-8) and (b) synthesized MOF (ZIF-8). The diffraction peaks of synthesized MOF sample are in indexed as cubic structure with an I-43 m(217) space group (CCDC number: 602542). The positions and relative intensity of all diffraction peaks match well with simulated MOF. No other impurity peaks are detected, indicating the highly crystalline structure of pure MOF.
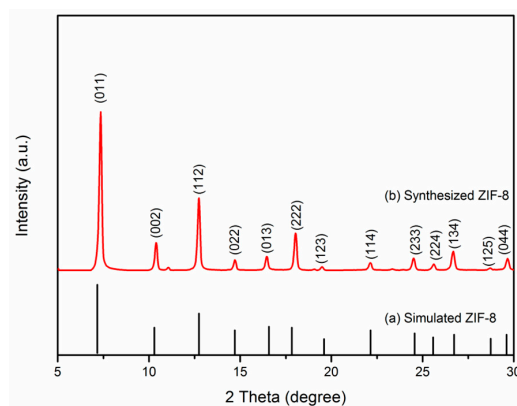


**Figure 1.** XRD patterns of (**a**) simulated MOF (ZIF-8) and (**b**) synthesized pure MOF (ZIF-8).

Figure 2 shows the XRD patterns of MOF/BiFeO$_3$ composite samples. The diffraction peaks of MOF/BiFeO$_3$ composite in Figure 2b are identified as a perovskite based rhombohedral structure with an R3c space group (JCPDS No. 86-1518) along with the existence of minority phase such as Bi$_2$Fe$_4$O$_9$. It is interesting to note that the composite with MOF does not change the phase structure of BiFeO$_3$, and the composite still exhibits almost the same purity and crystallinity as the pure BiFeO$_3$ shown in Figure 2a.
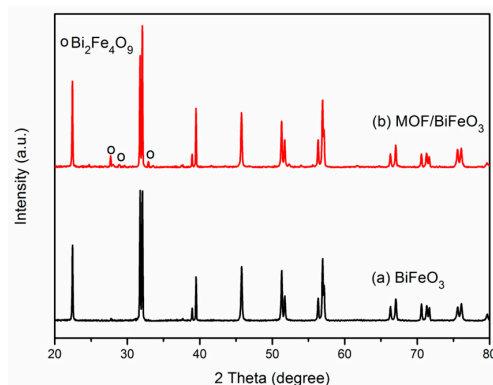


**Figure 2.** XRD patterns of (**a**) pure BiFeO$_3$ and (**b**) MOF/BiFeO$_3$.

### 3.2. Morphology and Microstructure Analysis

　　As seen in Figure 3a, spherical $BiFeO_3$ particles are prepared by a hydrothermal process. Furthermore, no other morphologies can be detected, indicating a high uniformity of the product with the spherical morphology. The magnification of pure $BiFeO_3$ shown in Figure 3b,c, spherical $BiFeO_3$ are formed by the aggregation of many microcubes, which is consistent with a previous report [17]. It is clear that the surface morphology of $BiFeO_3$ particle is very smooth in Figure 3c, which may be one of the reasons for the poor adsorption ability of the pure $BiFeO_3$. Figure 3d shows the SEM images of prepared MOF (ZIF-8), pure MOF particles exhibit regular spherical morphology with an average diameter of 60~80 nm. SEM images of MOF/$BiFeO_3$ composite in Figure 4a–d show lamellar MOF well disperse on the surface of $BiFeO_3$ particle, the surface morphology of MOF/$BiFeO_3$ composite changes obviously compared with the pure $BiFeO_3$. The particle surface is coarse and porous, which allows the organic molecules to adsorb on the catalyst surface more easily and provide more reactive sites. These will contribute to the increase of the reactive sites, as well as the enhanced separation efficiency of the photogenerated electron–hole pairs.
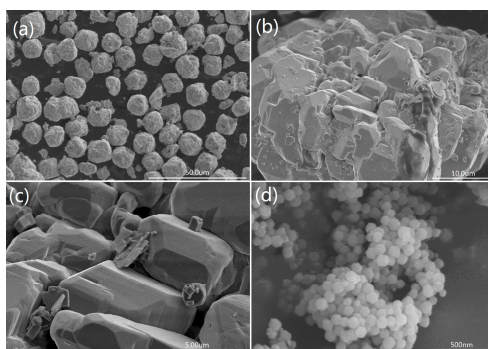


**Figure 3.** SEM images of (**a**) pure $BiFeO_3$; (**b**,**c**) the magnification of pure $BiFeO_3$; and (**d**) pure MOF.
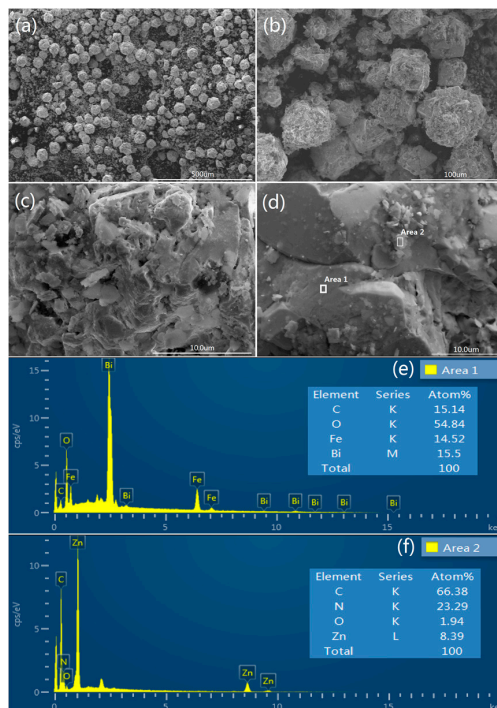


**Figure 4.** SEM images of (**a**) MOF/$BiFeO_3$ composite; (**b**–**d**) the magnification of MOF/$BiFeO_3$ composite. EDS spectrum of MOF/$BiFeO_3$ composite, (**e**) Area 1, (**f**) Area 2.

Energy dispersive spectroscopy (EDS) analysis was carried out to identify the components of MOF/BiFeO$_3$ composite. Figure 4e shows the diffraction peaks of Bi, Fe, O, and C elements corresponding to MOF/BiFeO$_3$ composite observed in area 1 marked in Figure 4d. From the insert table in Figure 4e, it can be seen that the experimental atomic ratio of Bi, Fe, and O elements is close to the theoretical one of pure BiFeO$_3$. A small amount of C element was detected and should be the result of a small amount of MOF adhering to the surface of the BiFeO$_3$. Figure 4f shows the element contents of Area 2 marked in Figure 4d. The ratio of the elements in the insert table is close to the theoretical ZIF-8 and confirms that the lamellar MOF was successfully dispersed on the surface of BiFeO$_3$ particle.

## 3.3. Enhanced Photocatalytic Performance

The photocatalytic activity of pure BiFeO$_3$, pure MOF, and MOF/BiFeO$_3$ composite photocatalysts under visible light irradiation were defined by measuring the photodegradation of MB aqueous solution. Where C$_0$ and C are the initial and final concentration of MB, respectively. After 100 min of visible light irradiation, the maximum percentage of dye decomposition increased from 78% for pure BiFeO$_3$ to 93% for MOF/BiFeO$_3$ composite photocatalyst, as shown in Figure 5d. As a contrast, when pure MOF powders of the same amount were added to the photocatalytic experiments in Figure 5b, they absorbed about 48% of the dye in the dark environment for 30 min, and hardly underwent photocatalytic reactions under light irradiation. Degradation experiments showed that MOF has no photocatalytic capacity, despite excellent adsorption properties. After 40 min, dye adsorption reached the maximum, 50% of the MB dye was adsorbed. As shown in Figure 5a,c, compared with pure BiFeO$_3$, the enhancement of MB photodegradation efficiency for MOF/BiFeO$_3$ composite photocatalyst was mainly thanks to the promotion of adsorption capability. Approximately 32% MB was absorbed by composite photocatalyst in the first 30 min. However, for pure BiFeO$_3$, only 1.5% was absorbed. The results of degradation experiments confirmed that the change of the surface morphology of the MOF/BiFeO$_3$ composite photocatalyst can effectively enhance the photocatalytic degradation ability of MB molecules.
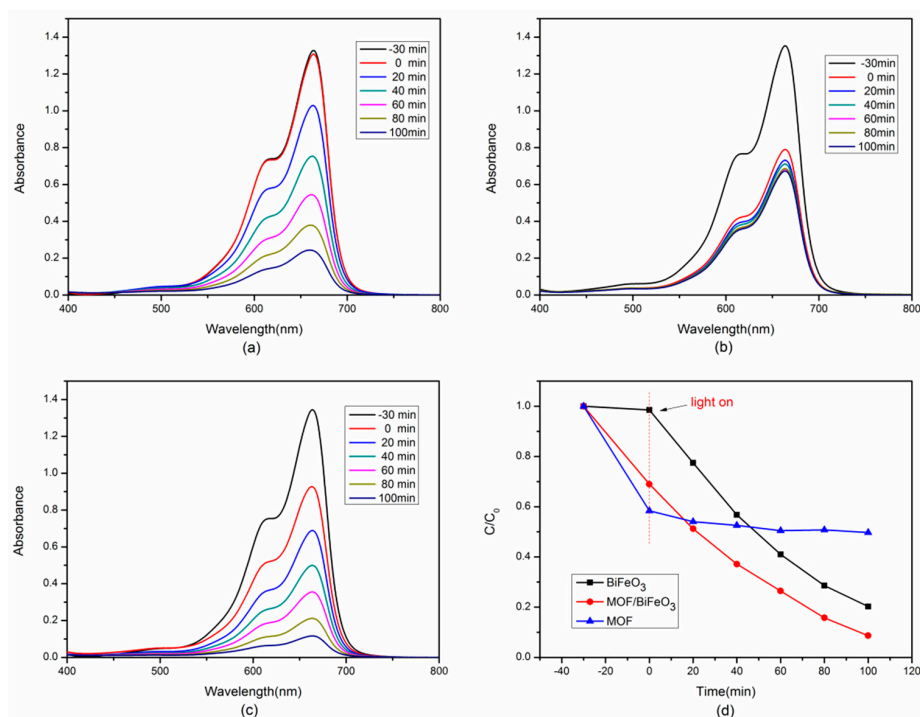


**Figure 5.** Time dependent UV–vis spectrum changes of MB catalyzed by (**a**) pure BiFeO$_3$; (**b**) pure MOF; and (**c**) MOF/BiFeO$_3$ composite; (**d**) The photocatalytic degradation efficiencies of all samples to degrade MB.

### 4. Photocatalytic Reaction Mechanism of MB over MOF/BiFeO$_3$ Composite

Under the irradiation of visible light, MOF/BiFeO$_3$ composite photocatalyst can effectively absorb photons thanks to its narrow band gap. The photocatalytic process included a series of photochemical reactions through the first step of electrons (e$^-$) and holes (h$^+$) generation (Figure 6). The photogenerated holes in the valence band (VB) combine with absorbed H$_2$O molecules to form strong oxidized hydroxyl radical (OH). In the presence of dissolved O$_2$, the electrons in the conduction band (CB) can react with O$_2$ to form superoxide radical (O$_2{}^-$) and hydrogen peroxide (H$_2$O$_2$). The OH radical has been deliberated to be the key active species accountable for the BiFeO$_3$ photocatalytic process. The holes can also directly react with organic pollutants adsorbed on MOF/BiFeO$_3$ composite and oxidize it to CO$_2$ and H$_2$O. The proposed mechanism (1–8) is as follows:

1. Absorption of efficient photons by MOF/BiFeO$_3$ composite photocatalyst

$$(\text{MOF/BiFeO}_3) + h\nu \rightarrow e^-_{CB} + h^+_{VB} \tag{1}$$
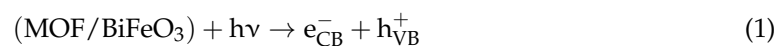
2. Holes (h$^+$) in valence band combine with absorbed H$_2$O molecules which produces hydroxyl radical (·OH)

$$h^+ + H_2O \rightarrow \bullet OH + H^+ \tag{2}$$
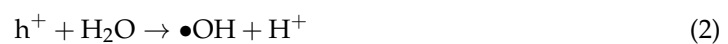
3. Oxygen ionosorption

$$O_2 + e^- \rightarrow \bullet O_2^- \tag{3}$$

4. Neutralization of by $\bullet O_2^-$ protons

$$\bullet O_2^- + H^+ \rightarrow \bullet OOH \tag{4}$$
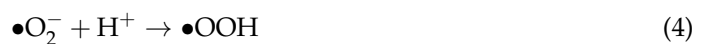
5. Transient hydrogen peroxide formation and dismutation of oxygen

$$2\bullet OOH \rightarrow O_2 + H_2O_2 \tag{5}$$

6. Decomposition of hydrogen peroxide

$$H_2O_2 + e^- \rightarrow \bullet OH + OH^- \tag{6}$$

7. Hydroxyl radical is further generated

$$H_2O_2 + \bullet O_2^- \rightarrow \bullet OH + OH^- + O_2 \tag{7}$$
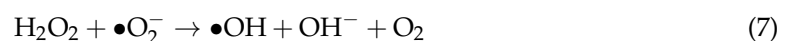
8. Oxidation of the MB molecules via successive attacks by ·OH and direct oxidation by reaction with holes

$$MB + \bullet OH,\ h^+ \rightarrow CO_2 + H_2O + \cdots\cdots \tag{8}$$
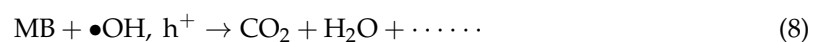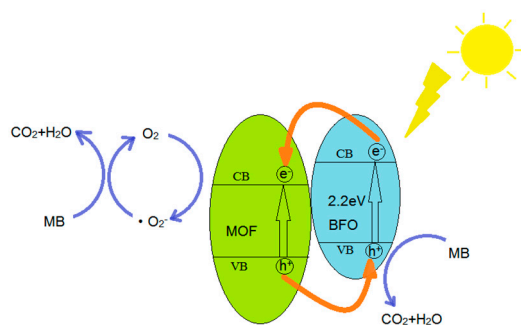
**Figure 6.** Schematic diagram for photocatalytic degradation of MB.

## 5. Conclusions

In this work, a novel MFO/BiFeO$_3$ composite photocatalyst with high photocatalytic efficiency has been successfully synthesized through a hydrothermal method. Characterization of the composite photocatalyst confirmed that the MOF with strong adsorptive property was successfully immobilized on the BiFeO$_3$ structure. The surface morphology of MOF/BiFeO$_3$ composite changed obviously compared with the pure BiFeO$_3$, a large surface area increased the number of active sites to promote the separation of e$^-$ and h$^+$ pairs and improved the light absorption ability owing to multiple scattering effect. According to the degradation of MB, the introduction of MOF can enhance the adsorption capacity of BiFeO$_3$ effectively, thereby enhancing the degradation of MB under visible light irradiation. This work proposed a new idea for efficient photocatalysts that can be used for purification of industrial waste.

**Author Contributions:** Yayun Li conceived and designed the experiments; Yunhui Si performed the experiments and wrote the manuscript; Jizhao Zou, Xinbo Xiong, Xierong Zeng and Ji Zhou helped perform the analysis with constructive discussions.

**Conflicts of Interest:** The authors declare no conflict of interest.

## References

1. Abe, R. Recent progress visible light irradiation on photocatalytic and photoelectrochemical water splitting under visible light irradiation. *J. Photochem. Photobiol. C* **2010**, *11*, 179–209. [CrossRef]
2. Xu, J.H.; Wang, W.Z.; Sun, S.M.; Wang, L. Enhancing visible-light-induced photocatalytic activity by coupling with wide-band-gap semiconductor: A case study on Bi$_2$WO$_6$/TiO$_2$. *Appl. Catal. B Environ.* **2012**, *111*, 126–132. [CrossRef]
3. Devi, L.G.; Kavitha, R. A review on nonmetal ion doped titania for the photocatalytic degradation of organic pollutants under UV/solar light: Role of photogenerated charge carrier dynamics in enhancing the activity. *Appl. Catal. B Environ.* **2013**, *140*, 559–587. [CrossRef]
4. Gao, F.; Chen, X.Y.; Yin, K.B.; Dong, S.; Ren, Z.F.; Yuan, F.; Yu, T.; Zou, Z.G.; Li, J.M. Visible-light photocatalytic properties of weak magnetic BiFeO$_3$ nanoparticles. *Adv. Mater.* **2007**, *19*, 2889–2892. [CrossRef]
5. Xue, Z.H.; Wang, T.; Chen, B.D.; Malkoske, T.; Yu, S.L.; Tang, Y.L. Degradation of tetracycline with BiFeO$_3$ prepared by a simple hydrothermal method. *Materials* **2015**, *8*, 6360–6378. [CrossRef] [PubMed]
6. Guo, R.Q.; Fang, L.; Dong, W.; Zheng, F.G.; Shen, M.G. Enhanced photocatalytic activity and ferromagnetism in Gd doped BiFeO$_3$ nanoparticles. *J. Phys. Chem. C* **2010**, *114*, 21390–21396. [CrossRef]
7. Zhang, X.; Wang, B.; Wang, X.; Xiao, X.; Wu, Z.W.; Zheng, J.; Ren, F.; Jiang, C.Z. Preparation of M@BiFeO$_3$ nanocomposites (M = Ag, Au) bowl arrays with enhanced visible light photocatalytic activity. *J. Am. Ceram. Soc.* **2015**, *98*, 2255–2263. [CrossRef]

8.  Wang, B.; Wang, S.M.; Gong, L.X.; Zhou, Z.F. Structural, magnetic and photocatalytic properties of $Sr^{2+}$-doped $BiFeO_3$ nanoparticles based on an ultrasonic irradiation assisted self-combustion method. *Ceram. Int.* **2012**, *38*, 6643–6649. [CrossRef]

9.  Chauhan, S.; Kumar, M.; Chhoker, S.; Katyal, S.C.; Singh, H.; Jewariya, M.; Yadav, K.L. Multiferroic, magnetoelectric and optical properties of Mn doped $BiFeO_3$ nanoparticles. *Solid State Commun.* **2012**, *152*, 525–529. [CrossRef]

10. Hu, C.; Wang, Y.; Tang, H. Influence of adsorption on the photodegradation of various dyes using surface bond-conjugated $TiO_2$ /$SiO_2$ photocatalyst. *Appl. Catal. B Environ.* **2001**, *35*, 95–105.

11. Oshikiri, M.; Boero, M.; Matsushita, A.; Ye, J. Water adsorption onto Y and V sites at the surface of the $YVO_4$ photocatalyst and related electronic properties. *J. Chem. Phys.* **2009**, *131*, 034701. [CrossRef] [PubMed]

12. Liu, X.; Guo, W.; Lu, Z.; Huo, P.; Yao, G.X.; Yan, Y.S. Surface molecular imprinting modified $TiO_2$ photocatalyst for adsorption and photocatalytic degradation of salicylic acid. *Fresen. Environ. Bull.* **2014**, *23*, 1626–1634.

13. Eddaoudi, M.; Kim, J.; Rosi, N.; Vodak, D.; Wachter, J.; O'Keeffe, M.; Yaghi, O.M. Systematic design of pore size and functionality in isoreticular MOFs and their application in methane storage. *Science* **2002**, *295*, 469–472. [CrossRef] [PubMed]

14. Duren, T.; Sarkisov, L.; Yaghi, O.M.; Snurr, R.Q. Design of new materials for methane storage. *Langmuir* **2004**, *20*, 2683–2689. [CrossRef] [PubMed]

15. Kuesgens, P.; Rose, M.; Senkovska, I.; Fröde, H.; Henschel, A.; Siegle, S.; Kaskel, S. Characterization of metal organic frameworks by water adsorption. *Microporous Mesoporous Mater.* **2009**, *120*, 325–330. [CrossRef]

16. Wang, Y.G.; Xu, G.; Ren, Z.H.; Wei, X.; Weng, W.J.; Du, P.Y.; Shen, G.; Han, G.R. Mineralizer-assisted hydrothermal synthesis and characterization of $BiFeO_3$ nanoparticles. *J. Am. Ceram. Soc.* **2007**, *90*, 2615–2617. [CrossRef]

17. Li, S.; Lin, Y.H.; Zhang, B.P.; Nan, C.W.; Wang, Y. Photocatalytic and magnetic behaviors observed in nanostructured $BiFeO_3$ particles. *J. Appl. Phys.* **2009**, *105*. [CrossRef]